Evaluation of Selected Wyoming Silica Sand Deposits as Potential Sources of Proppant

Andrea M. Loveland and James R. Rodgers

Report of Investigations 75 • 2017

WYOMING STATE GEOLOGICAL SURVEY
Erin A. Campbell, Director and State Geologist

Director and State Geologist Erin A. Campbell

Design and layout by:
Christina D. George
and Andrea M. Loveland

Evaluation of Selected Wyoming Silica Sand Deposits as Potential Sources of Proppant

Wyoming State Geological Survey Report of Investigations 75, 2017

Citation: Loveland, A.M., and Rodgers, J.R., 2017, Evaluation of selected Wyoming silica sand deposits as potential sources of proppant: Wyoming State Geological Survey Report of Investigations 75, 22 p.

Cover photo: Killpecker Dunes in Sweetwater County, Wyoming. Photo by Andrea M. Loveland, WSGS, 2017.

Evaluation of Selected Wyoming Silica Sand Deposits as Potential Sources of Proppant

Wyoming State Geological Survey
Report of Investigations 75
2017

Andrea M. Loveland and James R. Rodgers

Wyoming State Geological Survey, Laramie, Wyoming 82071

Table of Contents

List of Figures

List of Tables

List of Tables in the Appendices

ABSTRACT

Industrial sands are high in silica content and widely used in hydraulic fracturing, the manufacture of ceramics and glass, foundry applications, construction, and filtration processes. Currently, the highest demand (>70 percent) is for hydraulic fracturing proppants in the oil and gas industry. Transportation costs are expensive, therefore locating a sand source in proximity to areas of petroleum production is advantageous.

The Wyoming State Geological Survey (WSGS) collected sand samples from bedrock, aeolian dune, and alluvial fan deposits throughout Wyoming to evaluate their suitability for use in hydraulic fracturing. Two independent laboratories tested the samples for silica content, grain size, sphericity and roundness, turbidity, acid solubility, and crush resistance.

Sand deposits analyzed in this study have negligible or limited economic potential for use in hydraulic fracturing but may have potential in other industrial sand markets given their high silica content and relatively low levels of impurities.

INTRODUCTION

Industrial sands are high-purity silica (SiO_2) sands with well-sorted grain size distributions. Depending on chemical composition, mineralogy, and other physical characteristics, industrial sands are widely used in hydraulic fracturing, the manufacture of ceramics, glass and highly purified free silicon, foundry applications, sand blasting, and industrial filtration processes (fig. 1).

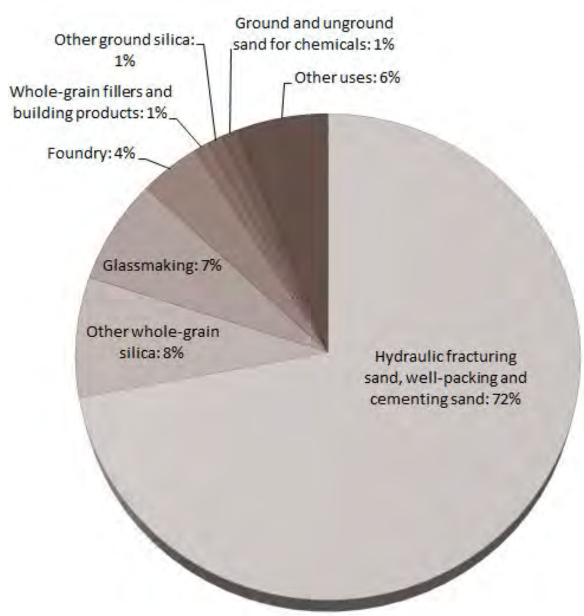

Figure 1. Domestic industrial sand end-uses in 2016 (modified from Dolley, 2017).

The United States is the largest producer of industrial sand and gravel, accounting for 51 percent of global production in 2016 (Dolley, 2017). The ten top producing states in order by tonnage are Wisconsin, Illinois, Texas, Missouri, Minnesota, North Carolina, Michigan, Oklahoma, Louisiana, and Arkansas. In 2016, these states produced 82 percent of the domestic total (Dolley, 2017).

For this study, the WSGS collected silica sand samples throughout Wyoming to evaluate their suitability for use in hydraulic fracturing. Seventeen samples were collected from Quaternary dune sand/loess and alluvial fan deposits (fig. 2). Seven additional samples were collected from areas previously studied by the WSGS (Harris, 1988a,b; Harris and Warchola, 1992; fig. 2). All samples were submitted to independent laboratories for analysis based on International Organization for Standardization (ISO) and American Petroleum Institute (API) fracturing (frac) sand properties because of the high percentage of use of silica sand for that purpose (fig. 1), although other uses were considered.

Properties of ideal frac sand deposits include high silica (> 95 percent) content, medium to coarse grain size, sphericity and roundness ≥0.6, low acid solubility, low turbidity, high crush resistance (≥ 5,000 psi), and proximity to transportation systems that serve hydrocarbon basins (API, 2008; Zdunczyk, 2014).

PREVIOUS WORK

Previous WSGS reports evaluated silica content and estimated volume of resources in selected Wyoming silica sand deposits. Harris (1988a) quantified silica content and the main impurities within Pennsylvanian–Permian Casper Formation samples from outcrop and boreholes drilled at the Plumbago Creek deposit in Albany County. Harris (1988a) estimated the 480-ft-thick Plumbago Creek deposit contains 64 million tons of silica sand.

Harris (1988b) also examined surface and subsurface samples from a 15- to 26-ft-thick upper orthoquartzite and an 18-ft-thick lower orthoquartzite in the Cretaceous Cloverly Formation at the Cassa silica sand deposit in Platte County. His report estimated that the deposit contains more than 72 million tons of high-grade silica sand with resource potential for glassmaking and other uses.

Harris and Warchola (1992) investigated the potential of the Tensleep Sandstone (Pennsylvanian) silica sand deposit in John Blue Canyon, Big Horn County. The exposure in John Blue Canyon has an average thickness of 20 ft. Silica

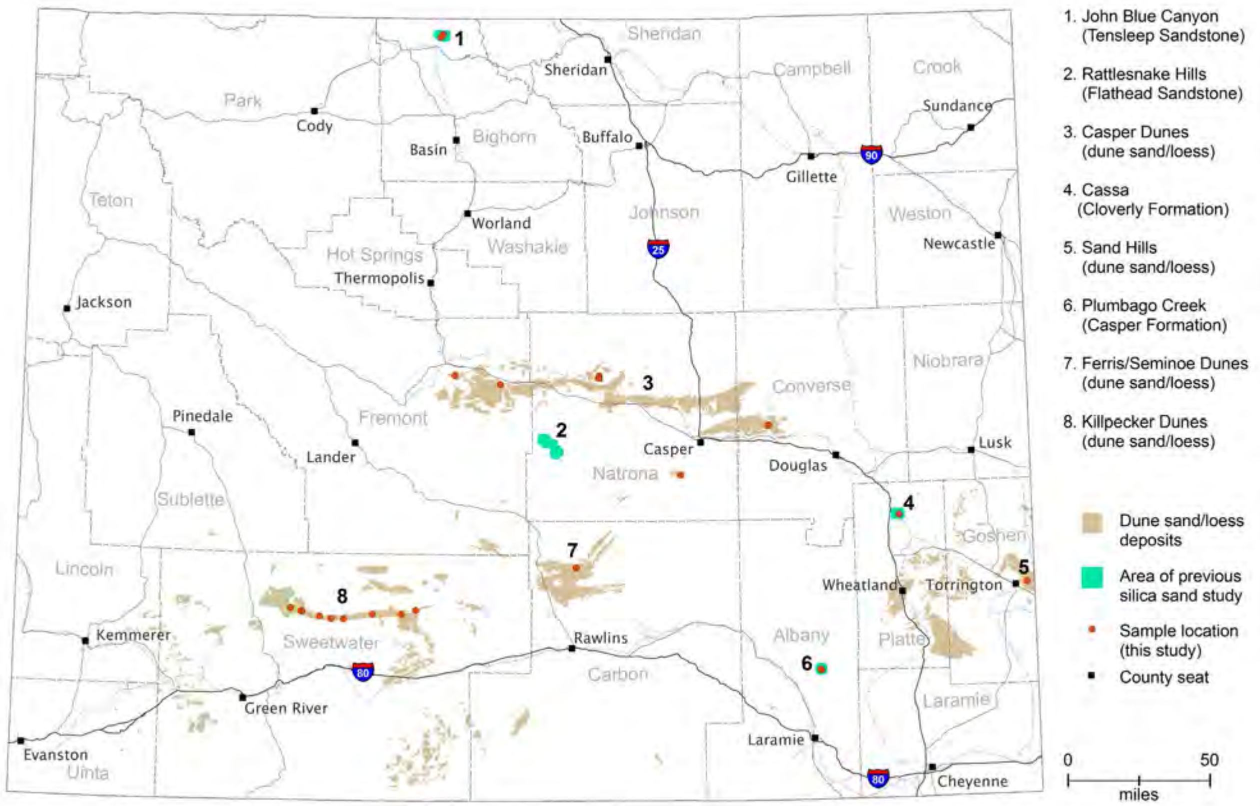

Figure 2. Map of sample locations and previous study areas within Wyoming. The distribution of Quaternary dune sand/loess from Love and Christiansen (1985) is shown as brown polygons.

reserves in this deposit are estimated at 169,083,000 tons. The report concludes that the fine-grained sand in this deposit may be a useful source for fused silica.

An unpublished report by Burlington Northern Railroad (Christiansen and Anderson, 1982) explored the potential of the upper and lower units of Cambrian Flathead Sandstone outcrops in the Rattlesnake Hills of the Wind River Basin. Based on outcrop observations and qualitative microscope analysis of sample composition, Christiansen and Anderson (1982) reported that the lower sandstone unit shows high potential as a silica sand deposit.

METHODS

Sampling

Outcrop sample collection was conducted during the 2015–2017 field seasons. Samples from the John Blue Canyon, Plumbago Creek, and Cassa deposits were collected from locations based on legal land descriptions of exposures provided by Harris and Warchola (1992) and Harris (1989a, b). New sample locations targeted aeolian dune deposits. Review of Love and Christiansen's (1985) geologic map of the state provided target locations of Quaternary dune sand/loess deposits; the Killpecker Dunes, Ferris-Seminoe Dunes, Casper Dunes, and Sand Hill Dunes were selected for sampling (fig. 2).

Lithified material was extracted from outcrop with a rock hammer. Unconsolidated and poorly consolidated sand deposits were collected by digging 1.5 to 2 ft down from the ground surface in order to retrieve sand with minimal potential contaminants and organic material. Roughly 10 lbs of sand or sandstone material was collected for each sample.

Sand Characterization

Sampling locations were chosen based on accessibility, land ownership status, and proximity to transportation routes. Because of the demand for domestic frac sands, samples were analyzed for their viability as hydraulic fracturing proppants (as opposed to other potential end-uses) utilizing testing procedures set by the ISO and API.

Initial tests were conducted by the University of Wyoming Department of Geology & Geophysics Petrology Laboratory (UWGGPL), based on API RP 19C/ISO 13503-2 (API and others, 2008) procedural specifications for testing hydraulic fracturing proppants. Samples were tested in a sequential, pass/fail manner; if a sample met criteria for a standard, it would be analyzed for the next standard, and if not, no further testing was conducted on that sample.

After disaggregating lithified samples in hydrochloric acid, a sequence of tests outlined below were performed.

Composition

Sands were analyzed for mineralogical composition. Quartz-feldspar-lithic (QFL) fragment analyses were performed using a reflected light microscope. Ideal frac sands have silica content greater than 95 percent, however, in many cases impurities can be processed out, significantly increasing the silica content. Therefore, samples containing ≥75 percent SiO_2 continued to the next phase of testing.

Geochemical data from previous studies were analyzed using box plots to show the range of silica content and identify any outlier data that may not be representative of the sample.

Grain Size and Shape

Grain size was determined in one of two ways: 1) by optical grain sizer (Microtrac Dynamic Image Analyzer™ (DIA)) for samples that disaggregated in hydrochloric acid solution, or 2) by reflected light microscope for samples that did not disaggregate. Samples with median grain sizes between 210 and 841 µm met size criteria for this study.

Grain shape was determined optically from the Microtrac DIA. Grains with greater roundness and sphericity provide better porosity and permeability when used as proppant. Therefore, samples demonstrating sphericity and roundness ≥0.6 on the Krumbein and Sloss chart (fig. 3) were deemed suitable for further testing.

Turbidity

Turbidity analysis verifies the amount of fine-grained particles, such as silt or clay, present in a sample by measuring the scattered light of particles suspended in a formazin-based solution. For frac sands, low turbidity is desirable, although this property can be controlled to an extent by washing out fine-grained material during processing (Zdunczyk, 2007). In this study, turbidity was measured in Formazin Turbidity Units (FTU); samples passed to the next level of testing if they yielded a turbidity value ≤250 FTU.

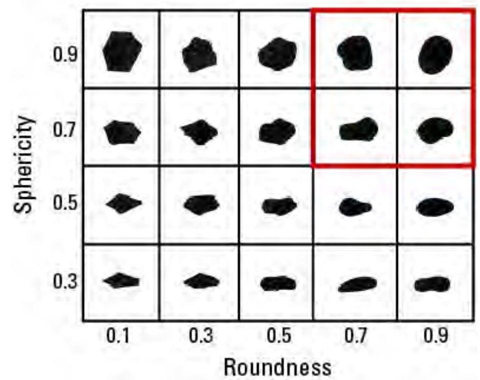

Figure 3. Krumbein-Sloss chart highlighting grain roundness and sphericity >0.6 in red (modified from Krumbein and Sloss, 1963).

Acid Solubility

Solubility of a sand depends on the amount of soluble cement and/or mineral grains it contains. Typically, sands with high silica content have low solubility. Acid solubility was tested by comparing the weight change in each sample after submerging them in reactant for 24 to 48 hours. Samples passed the acid solubility test if: 1) a maximum of two percent of sands between mesh size 6/12 and 30/50 were soluble in acid, or 2) a maximum of three percent of sands between mesh size 40/70 and 70/140 were soluble in acid.

Crush Resistance

An important characteristic of quality frac sand is the ability of individual grains to resist fracturing. Intact grains are necessary to keep fluid migration pathways open at various depths and temperatures (Benson and Wilson, 2015). Depending on depth, pressure, and well bore temperature, sands that fall within a range of mesh sizes and k-values (the pressure at which 10 percent or more of the grains break into fines) may be used. For example, coarser-grained sands (20/40 and 30/50 mesh) with k-values between two and four can be used for relatively shallow wells or softer source rock; 5k to 8k sands of the same mesh sizes would be more suitable for deeper wells (Bellmund, 2017; table 1).

For this study, samples that met the criteria for the previously summarized analytical tests were subsequently sent to Legend Technical Services, Inc. for crush resistance testing. Intervals of increasing pressure were applied to and held on disaggregated samples in accordance with API RP 19C/ISO 13502-2 specifications. After crushing at a pressure

Table 1. Crush resistance classification chart showing mesh sizes and the corresponding range of stresses and k-values that are viable for hydraulic fracturing (modified from American Petroleum Institute, 2008; Bellmund, 2017).

<table>
<tr><th colspan="2">Mesh Size</th><th>Stress (psi)</th><th>10% Crush Classification (k-value)</th></tr>
<tr><td></td><td></td><td>1,000</td><td>1k</td></tr>
<tr><td rowspan="7">20/40
30/50</td><td></td><td>2,000</td><td>2k</td></tr>
<tr><td rowspan="11">40/70
50/140 (100)</td><td>3,000</td><td>3k</td></tr>
<tr><td>4,000</td><td>4k</td></tr>
<tr><td>5,000</td><td>5k</td></tr>
<tr><td>6,000</td><td>6k</td></tr>
<tr><td>7,000</td><td>7k</td></tr>
<tr><td>8,000</td><td>8k</td></tr>
<tr><td></td><td>9,000</td><td>9k</td></tr>
<tr><td></td><td>10,000</td><td>10k</td></tr>
<tr><td></td><td>11,000</td><td>11k</td></tr>
<tr><td></td><td>12,000</td><td>12k</td></tr>
<tr><td></td><td>13,000</td><td>13k</td></tr>
</table>

appropriate for grain size (per API/ISO standards), samples were sieved to assess the percentage of resulting fine material. Sands that yielded <10 percent fines passed the crush resistance test and were again crushed at an increased pressure. Through this systematic process, the k-value of the sand was determined.

To assess the repeatability of crush test results, samples that met criteria were resampled in the field and analyzed by Legend Technical Services, Inc. First, acid solubility was evaluated; only samples that met solubility criteria were tested for crush resistance.

LOCATION DESCRIPTIONS AND RESULTS

Bedrock Deposits

Three bedrock deposits previously studied for geochemistry by WSGS geologists (Harris, 1988a, b; Harris and Warchola, 1992) were resampled and analyzed to further characterize their physical properties and assess their potential for use as hydraulic fracturing proppants. Table 2 summarizes the results of tests conducted for this study on bedrock sandstone samples.

John Blue Canyon Deposit—Big Horn County

The John Blue Canyon silica sand deposit is located in north-central Wyoming on the western flank of the Bighorn Mountains. Outcrop exposures of Pennsylvanian Tensleep Sandstone are located approximately 10 miles northeast of the town of Lovell in T. 57 N., R. 94 W., secs. 13, 14, 15, 23, 24, and in T. 57 N., R. 93 W., secs. 18 and 19 in the Natural Trap Cave and Simmons Canyon 1:24,000 quadrangles. It is accessible via Alternate U.S. Highway 14 on the east side of Bighorn Lake.

The Tensleep Sandstone in this area is a gray-white to purple, fine-grained, friable sandstone that averages only 20 ft thick (fig. 4). Weathered material from overlying units commonly covers exposures of the Tensleep Sandstone, making it difficult to locate in the field. It is typically thicker in other areas in the Bighorn Mountains; in this location, the thinning may represent the northern edge of a sand dune facies (Harris and Warchola, 1992).

Table 2. Table summarizing characteristics of bedrock sandstone samples analyzed in this study.

Location	Formation	Sample	Composition[1] (%)			Median Grain Size[2] (µm)	Mean Sphericity[3]	Turbidity (FTU)[4]	Acid Solubility[5] (%)
			Q	F	L				
John Blue Canyon	Tensleep Sandstone	20160823AML014	95	0	5	196.61	0.828	-	-
		20160823AML015a	85	10	5	100.86	0.805	-	-
		20160823AML015b	85	5	10	107.70	0.810	-	-
Cassa	Cloverly Formation	20160913AML016a	90	5	5	176.98	0.846	-	-
		20160913AML016b	95	2	3	100.00	-	-	-
Plumbago Creek	Casper Formation	20160822AML012	93	5	2	99.21	0.810	-	-
		20160822AML013b	95	2	3	108.20	0.836	-	-

[1]Composition greater than 70 percent silica; [2]Median grain size between 20 and 70 mesh (210 to 841 microns); [3]Mean sphericity ≥0.6; [4]Turbidity ≤250 FTU; [5]Acid solubility <3 percent

Harris and Warchola (1992) evaluated whole-rock geochemistry of Tensleep Sandstone samples collected as part of measured sections and one additional outcrop in the canyon, with results summarized in figure 5. Silica content ranges from 55 to 97 percent. The average of the mean values at each measured section is 87 percent. Based on assumptions regarding the thickness and lateral extent of the Tensleep Sandstone in this area, Harris and Warchola (1992) estimated that there may be 169,083,000 tons of silica sand at this site. However, overburden thickness is a consideration for potential economical excavation of these resources.

For this study, three samples were collected from outcrop exposures of the Tensleep Sandstone in John Blue Canyon on Bureau of Land Management (BLM) lands. Sample 20160823AML014 has a silica content of 95 percent with lithic fragments comprising the remainder of the sample (table 2). Sample 20160823AML015a has an SiO_2 content of 85percent, with feldspar composing the majority of impurities. Sample 20160823AML015b is also 85 percent silica, but lithic fragments constitute most of the impurities. The median grain size for each of these samples was below the testing threshold (101 and 108 µm, respectively). As such, these samples did not undergo further testing.

Figure 4. Thin exposure of friable Tensleep Sandstone in John Blue Canyon.

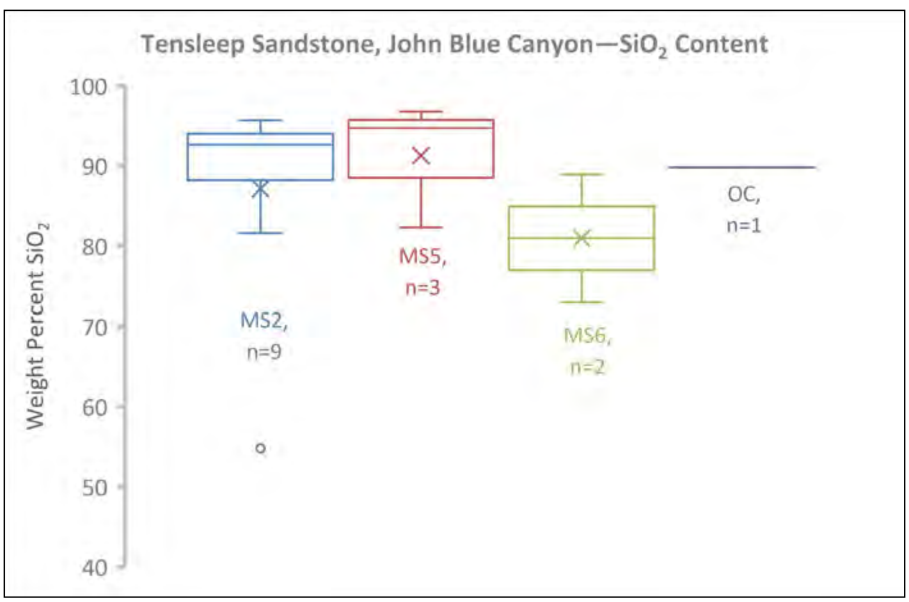

Figure 5. Box plot showing the silica content of Tensleep Sandstone samples collected from measured sections (MS) and outcrop (OC) in John Blue Canyon (data from Harris and Warchola, 1992).

Rattlesnake Hills Deposit—Natrona County

Rattlesnake Hills is a resource-rich area in the southwest corner of Natrona County in the Wind River Basin. The area is known for its uranium and gold deposits and hydrocarbon resources. A silica sand exposure composed of Cambrian Flathead Sandstone is located in the Ervay Basin SW and Garfield Peak 1:24,000 quadrangles within the Rattlesnake Hills 1:100,000 quadrangle (Sutherland and Hausel, 2003; Lynds and others, 2016).

The deposit can be reached from the south on Wyoming Highway 220 via the Natrona County Road 321 turnoff (Dry Creek Road). It can also be approached from the north off U.S. Highway 20/26 via Gas Hills Road (Natrona County Road 136) about 50 miles west of Casper.

The Flathead Sandstone, as described by Bell (1970), was deposited primarily as coastal sand along a continental margin during the Cambrian period as the sea encroached upon land. The formation has distinguishable lower and upper sub-units. The lower unit is a cross-bedded, well-cemented, medium-grained orthoquartzite. The upper unit exhibits parallel stratification of coarse- to fine-grained orthoquartzite that grades up section into interbedded clayey sandstone, siltstone, and shale.

This deposit was not sampled in this study, however, an unpublished report by Burlington Northern Railroad geologists (Christiansen and Anderson, 1982) evaluated outcrops of upper and lower sub-units in the Flathead Sandstone in the Rattlesnake Hills for industrial use potential. The lower sub-unit is described as a white to orange, buff- to red-brown-weathering quartz arenite. It is friable and well sorted with sub-angular to rounded grains. The upper sub-unit is a red-gray, red-brown-weathering quartz arenite that is well-sorted and displays a sub-rounded to rounded grain shape. Microscope analysis of grain size, shape, mineralogy, and friability was conducted by Christiansen and Anderson (1982) and results of the analyses are summarized in appendix 1.

The box plot in figure 6 shows the distribution of silica content based on the qualitative analysis of sample mineralogy (Christiansen and Anderson, 1982). The average silica content among the lower Flathead Sandstone samples was 97 percent. The minimum silica value, exclusive of outlier values, was 97 percent, and the maximum was 99 percent. The mean silica content for upper Flathead Sandstone samples was 95 percent. The minimum and maximum values, exclusive of outliers, was 95 and 99 percent, respectively.

Recent investigation into the viability of this deposit for use in hydraulic fracturing showed that these sands, although rich in silica, are marginal in roundness and sphericity, and yield low k-values (James Goodrich, written commun., 2017). For this reason, the Flathead Sandstone in the Rattlesnake Hills area was not resampled for this study.

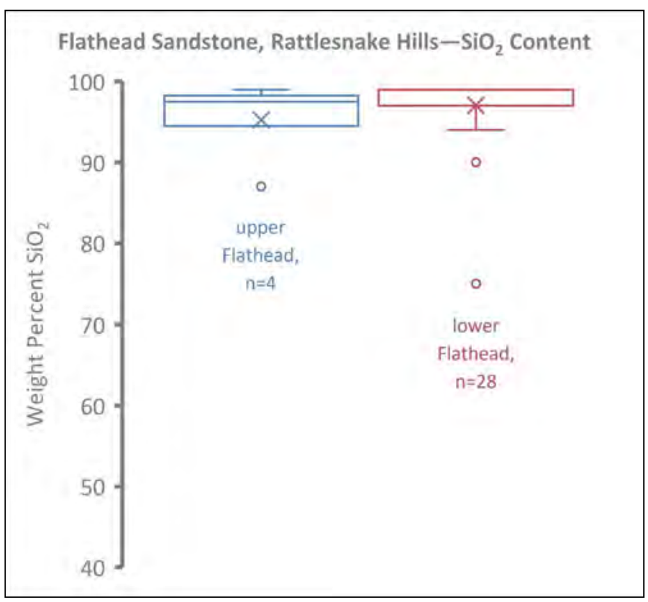

Figure 6. Box plot showing the silica content of upper and lower Flathead Sandstone samples from the Rattlesnake Hills area based on microscope analysis (Christiansen and Anderson, 1982).

Cassa Deposit—Platte County

The Cassa silica deposit is a Cretaceous Cloverly Formation sandstone located in Platte County about 5 miles southeast of Glendo. Outcrop exposures are accessible via Wyoming Highway 319 in T. 29 N., R. 68 W., secs 25, 26, 27, 34, 35, and 36 of the Sibley Peak and Cassa 1:24,000 quadrangles.

The Cloverly Formation in the study area is composed of fluvial or marginal marine orthoquartzite intervals separated by zones of silty sandstone, claystone, and cross-bedded fluvial sandstone (fig. 7). The formation ranges from 46 to 112 ft thick based on borehole measurements documented by Harris (1988b).

Previous investigation of the Cassa deposit evaluated upper and lower orthoquartzite intervals in the Cloverly Formation (Harris, 1988b). Whole-rock geochemistry performed on drill core samples indicated high silica content in both intervals. Harris' (1988b) data indicates that the upper orthoquartzite interval averages 98 percent SiO_2 and the lower interval averages 96 percent. Figure 8 shows the range in silica content of the upper and lower orthoquartzites combined. The mean SiO_2 content among the wells ranges from 88 to 94 percent. The average of the means in all six wells is 91 percent. Harris (1988b) also reported that there were negligible amounts of impurities such as iron, manganese, and chromium.

Two new samples were collected from state lands for this study from a Cloverly Formation exposure on a railroad cut adjacent to the North Platte River. Sample 20160913AML016a was collected from a light gray to white, very fine to fine-grained, thin-bedded sandstone. This sample consists of 90 percent silica, and five percent each of feldspar and lithic fragments (table 2). However, sample 20160913AML016a contains a significant amount of silica silt and cement; it did not meet the standard for favorable grain size.

Sample 20160913AML16b was collected from the overlying darker-colored, coarser-grained sandstone. It has a silica content of 95 percent and feldspar and lithic fragments (table 2). The median grain size for this sample was 100 μm; it did not align with standards for grain size and was not tested further.

Figure 7. South-facing view of Cloverly Formation outcrop along the North Platte River and the BNSF Railway in the Cassa deposit area.

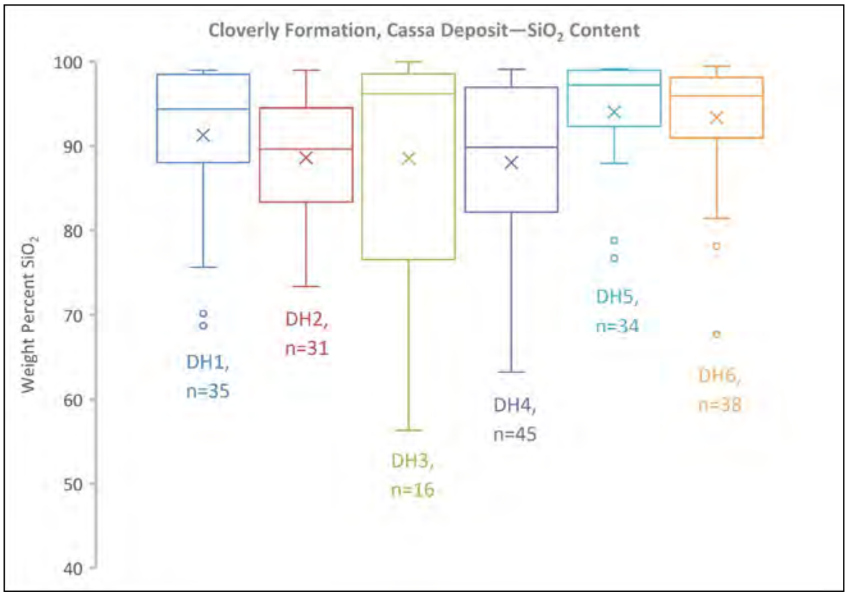

Figure 8. Box plot showing silica content of borehole samples from the Cassa deposit (data from Harris, 1988b).

Plumbago Creek Deposit—Albany County

The Plumbago Creek silica sand deposit is located off Wyoming Highway 34 on Albany County Road 12 in T. 20 N., R. 73 W., sec. 36 of the Sybille Springs 1:24,000 quadrangle. It is composed of the Pennsylvanian–Permian Casper Formation (fig. 9), originally described by Darton (1908) as a carbonate, sandstone, and shale sequence. The silica sand deposit at Plumbago Creek formed as wind-blown dunes in a beach environment. The sands contain intermittent carbonate interbeds, which indicate a transgressive-regressive cycle along a paleo shoreline (Harris, 1988a).

Harris (1988a) conducted a mapping and drilling project to assess the viability of the 480-ft-thick Plumbago Creek silica sand deposit for industrial uses. Six holes were drilled and sand samples from various depths were analyzed for whole-rock geochemistry to quantify silica content.

Figure 10 shows the silica content distribution of samples tested in each borehole. The plot includes data collected from sand intervals and excludes data from interbedded zones of dolomite or calcium carbonate. Collectively, the range in weight percent SiO_2 is 44 to 97 percent (excluding outliers). The average silica content in these wells range from 75 to 82 percent. The average of the mean values in all six boreholes is 77 percent. Harris (1988a) suggests that calcium carbonate accounts for 10 to 25 percent of impurities, which are removable by washing processes, potentially resulting in SiO_2 content of 95 percent or higher.

Two new samples of lithified outcrop collected from state lands at the Plumbago Creek site, 20160822AML012 and 20160822AML013b, yielded silica contents of 93 and 95 percent, respectively (table 2). Optical grain size analysis, however, revealed that the sands were too fine to meet testing criteria, so these samples did not undergo further analysis.

Figure 9. North-facing view of a Casper Formation exposure at Plumbago Creek.

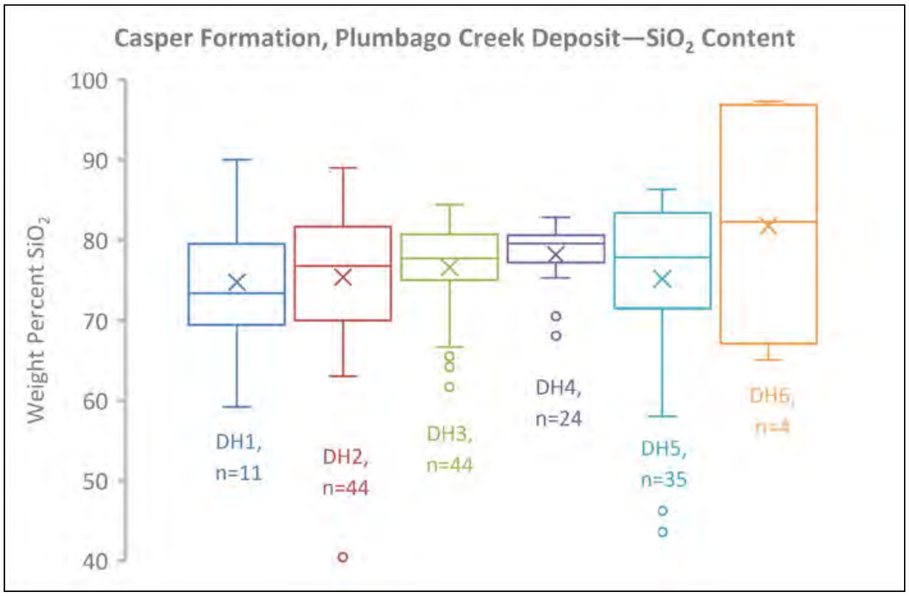

Figure 10. Box plot showing silica content from borehole samples in the Plumbago Creek deposit (data from Harris, 1988a).

Dune Sand/Loess and Alluvial Fan Deposits

Wyoming's sand dunes occur within and immediately adjacent to the Wyoming Wind Corridor (WWC) (Kolm, 1982; fig. 11). The WWC is an area of persistently western prevailing winds topographically bound by the Uinta, Sierra Madre, and Medicine Bow mountains to the south and the Wind River, Ferris, Seminoe, and Shirley mountains to the north (Kolm and Marrs, 1977; Marrs and others, 1987; Gaylord, 1989). The WWC extends 375 mi across the state from the Green River Basin on the west to the Nebraska Sand Hills on the eastern border in a 90- to 125-mi wide belt (Marrs and others, 1987). Active dune fields addressed in this study that lie in the WWC include the Killpecker Dunes, Ferris-Seminoe Dunes, and the Sand Hills Dunes (referred to as such in this study) on the eastern border of Wyoming. The stable (inactive) Casper Dunes are part of a secondary wind corridor that originates near the southern margin of the Absaroka Mountains and merges with the WWC (Kolm, 1982).

A summary of results from initial samples collected from dune sand/loess and alluvial fan deposits in the WWC are shown in table 3. Samples from Killpecker Dunes and the Casper Dunes qualified for crush resistance testing.

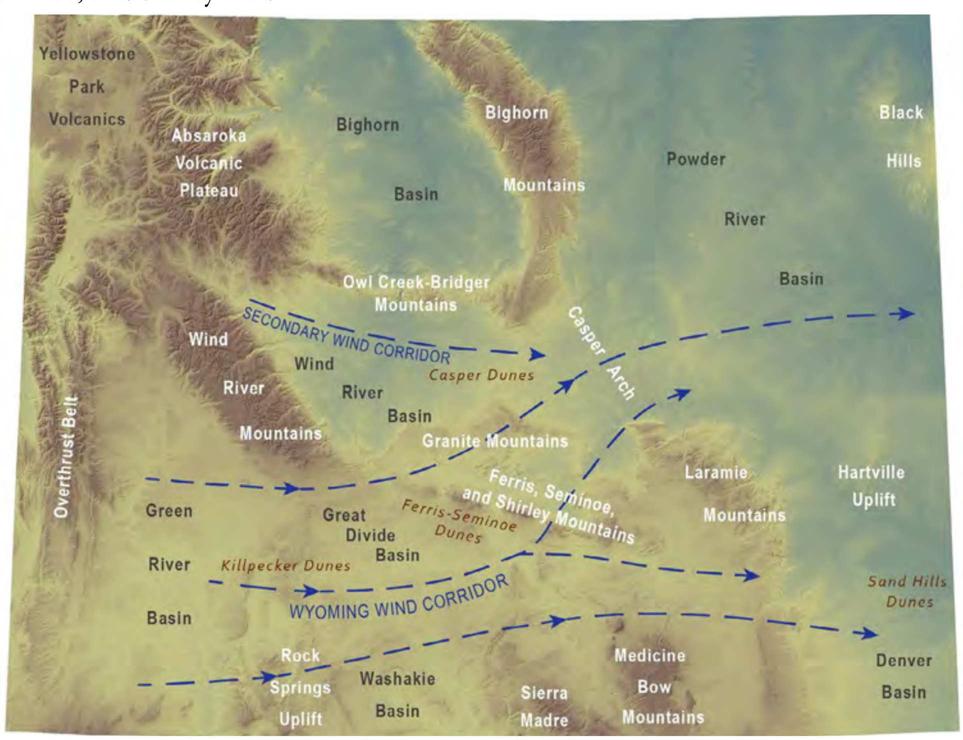

Figure 11. Physiographic map of Wyoming showing location of sand dunes within the Wyoming Wind Corridor (modified from Kolm and Marrs, 1977).

Table 3. Summary of dune sand/loess and alluvial fan characteristics from initial sampling.

Location	Formation	Sample	Composition[1] (%) Q	F	L	Median Grain Size[2] (μm)	Mean Sphericity[3]	Turbidity (FTU)[4]	Acid Solubility[5] (%)
Casper Dunes	Dune sand/ loess	20160721AML007	85	5	10	242.00	0.814	50	0.5
		20160721AML008	80	10	10	172.82	0.866		
	Alluvial fan	20160721AML009	85	5	10	231.02	0.855	250	1.6
	Dune sand/ loess	20160722AML010	85	5	10	269.79	0.888	920	0.9
		20160722AML011	90	5	5	339.59	0.850	375	-
Sand Hills	Dune sand/ loess	20151021AML001	85	5	10	108.83	0.866	-	-
Seminoe Dunes	Dune sand/ loess	20160627AML001	85	10	5	108.63	0.843	-	-
		20160627AML002	85	10	5	109.33	0.851	-	-
Killpecker Dunes	Dune sand/ loess	20160628AML004	75	5	20	287.61	0.880	230	1.7
		20160628AML005	75	5	20	120.65	0.872		
		20160628AML006	75	5	20	244.48	0.886	76	1.1

[1]Composition greater than 70 percent silica; [2]Median grain size between 20 and 70 mesh (210 to 841 microns);
[3]Mean sphericity ≥0.6; [4]Turbidity ≤250 FTU; [5]Acid solubility <3 percent

Casper Dunes/Alluvial Fan Deposit—Fremont, Natrona, and Converse Counties

The Casper Dunes consist of Quaternary dune sand/loess deposits located in the middle of the state along U.S. Highway 20/26 between Riverton and Glenrock (Love and Christiansen, 1985; fig. 11). The deposit spans approximately 125 mi from west to east across parts of the Riverton, Lysite, Midwest, Bill, Douglas, and Casper 1:100,000 quadrangles. The Casper Dunes sand is compositionally comparable to sediments from the North Platte River. Based on the similarity in geochemical signature, the Casper Dunes sand is likely sourced from fluvial deposits in the North Platte River valley (Albanese, 1974; Muhs, 2004).

Five samples were collected across the Casper Dunes. The quartz content of these samples ranges between 80 and 90 percent (table 3). This is consistent with the 81 to 84 percent silica reported by Muhs (2004).

Sample 20160721AML008 meets criteria for composition and shape, but is too fine for use as a hydraulic fracturing proppant. Samples 20160721AML007 and 0160721AML009, however, meet standards for composition, size, shape, turbidity, and acid solubility.

Sample 20160721AML007 was sieved to a 6/12 mesh cut and crushed at less than 1,000 psi. The sample is too weak for use as frac sand.

Unanswered questions regarding previous large-scale mapping in the central Casper Dunes area required further evaluation of the area from which sample 20160721AML009 was collected (fig. 12). Based on field observations and interpretation of aerial imagery, it was established that the sample was collected from an alluvial fan deposit rather than a dune deposit. The source of the alluvial fan is likely an adjacent exposure of the Frontier Formation. Nevertheless, it was sieved to a 40/70 mesh cut and held at an applied load of 4,000 psi. The resulting crushed material yielded eight percent fines. Therefore, this sample meets crush strength requirements for a 4k sand.

To test the repeatability of k-values, two additional samples were collected and analyzed for crush resistance, contingent on meeting criteria for acid solubility; one from the alluvial fan deposit and another from the easternmost dune deposit (fig. 13; appendix 2). Sample 20170606AML001 failed to meet acid solubility standards. Sample 20170607AML004, from the alluvial fan, qualifies as a 3k sand.

Figure 12. North-facing photograph of a Frontier Formation outcrop taken from a highly vegetated alluvial fan deposit in the Casper Dunes area.

Figure 13. Map showing the distribution of samples analyzed from the Casper Dunes and an alluvial fan deposit (20160721AML009). Initial sample locations (this study) are shown as yellow squares. Resampling locations are shown as red dots. K-values are displayed in brackets. The samples from the alluvial fan deposit show marginal potential for use as a low grade proppant. Locations without bracketed k-values did not undergo crush testing.

Sand Hills Dunes—Goshen County

Dune deposits located in eastern Goshen County are considered remnants of the Nebraska Sand Hills (Loope and Swinehart, 2000). Although not formally named Sand Hills in Wyoming, these deposits are referred to as such for the purposes of this study. The sand deposits are located near the town of Torrington off U.S. Highway 26 in the Torrington 1:100,000 quadrangle. Although no definitive source for the sand has been identified (Ahlbrandt and Freyberger, 1980), it is thought to originate from alluvial deposits (Stanley and Wayne, 1972).

One sample collected from state land in this area was analyzed (table 3). Although compositionally the sample is rich in silica, its grain size distribution was not adequate to proceed with further testing.

Ferris-Seminoe Dunes—Sweetwater and Carbon Counties

The Ferris-Seminoe Dunes are located within the Great Divide Basin in the WWC along the southern margin of the Ferris and Seminoe mountains in the Bairoil and Shirley Basin 1:100,000 quadrangles (fig. 11). The dunes (fig. 14) are accessible approximately 15 mi north of Rawlins off Wyoming Highway 789 (U.S. Highway 287).

Mineralogical analyses on potential sources of the sands at the Ferris-Seminoe Dunes suggest the main source comes from poorly lithified, arkosic sands from the Paleogene Battle Spring Formation (Gaylord, 1982). Minor sources originate from the easternmost tip of the Killpecker Dunes and from Cretaceous and Tertiary sandstones in the area (Gaylord, 1982).

Two new samples were collected from BLM lands at the Ferris-Seminoe Dunes. QFL analyses show that the quartz content of each sample is 85 percent (table 3). Although these samples meet the criteria for mineralogical composition, grain size is too fine and no further tests were performed.

Killpecker Dunes—Sweetwater County

The Killpecker Sand Dunes are located in the Greater Green River Basin of southwestern Wyoming in the SE Farson, NE Rock Springs, and N Red Desert Basin 1:100,000 quadrangles (fig. 11). The dunes trend east-west and extend for 55 miles across the eastern margin of the Green River Basin into the western Great Divide Basin. The dunes (fig. 15) are located in Sweetwater County and are accessible north of Rock Springs via U.S. Hwy 191 and Chilton Rd/Tri Territory Rd (County Road 4-17) or via the Point of Rocks exit off I-80 and County Road 15.

The dominant source of the Killpecker sand is the lacustrine Laney Member of the Eocene Green River Formation (Ahlbrandt, 1974). Although some coarse-grained material is deposited on the windward side of the dunes, the majority of grains range from fine to medium. This active dune field is unidirectional due to the prevailing west winds of the WWC (Ahlbrandt, 1973).

Initially, three new samples were collected from BLM lands at the Killpecker Dunes (fig. 16). The quartz content of each sample is 75 percent (table 3). In comparison, Merewether and others (1987) reported an average silica content of 79 percent, and Gibbons and others (1990)

Figure 14. North-facing view of the Ferris-Seminoe Dunes.

Figure 15. North-facing view of the Killpecker Dunes. The snow-capped Wind River Range is visible in the distance.

Figure 16. Map showing the distribution of samples analyzed from Killpecker Dunes. Initial sample locations (this study) are shown as yellow squares. Resampled locations are shown as red dots. K-values are displayed in brackets. Locations without bracketed k-values did not undergo crush testing.

reported an average of 77 percent on the western end of the dune field (fig. 17).

Samples 20160628AML04 and 20160628AML06 meet size and shape requirements, but sample 20160628AML05 is too fine grained. Samples 20160628AML04 and 20160628AML06 meet the criteria for turbidity and acid solubility (table 3).

Crush resistance results (appendix 2) indicate that sample 20160628AML04 has a crush classification of a 4k sand. Although this quality of sand is not viable for hydraulic fracturing in deep wells, it may have potential for shallow drilling applications. Sample 20160628AML06 is classified as an 8k sand. This implies that the sand has potential for use in hydraulic fracturing at greater depth and under higher pressures than sample 20160628AML04.

To test the repeatability of k-values, the dunes were resampled (fig. 16) and analyzed for crush resistance if they met criteria for acid solubility analysis (appendix 2). Sample 20170622AML011 is classified as a 3k sand; samples

20170622AML008 and 20170623AML012 do not meet acid solubility standards and therefore did not undergo crush resistance testing.

Figure 16 illustrates the lateral variation in the quality of these sands across a ~45 mile span and indicates that the repeatability of crush resistance across the Killpecker Dunes is poor.

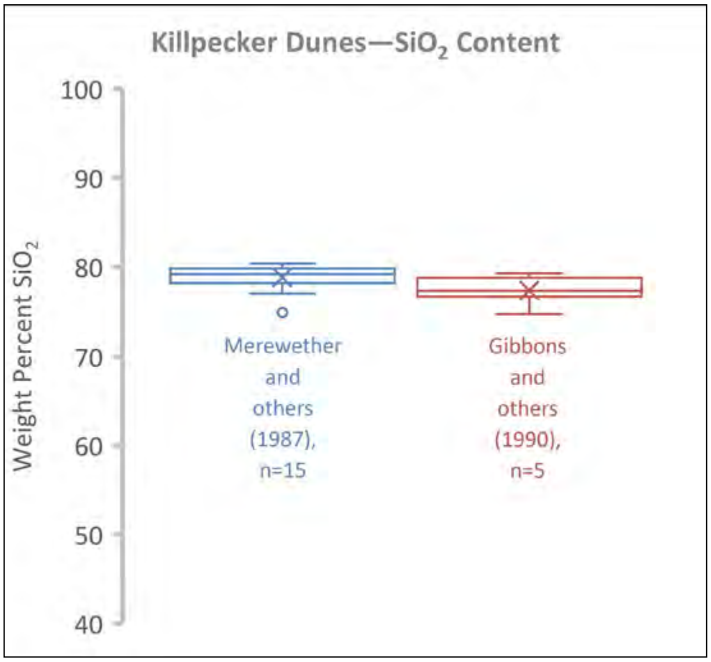

Figure 17. Box plot showing Killpecker Dune sands silica content from previous studies.

DISCUSSION

Bedrock Deposits

Bedrock silica sands analyzed in this study have negligible economic potential with respect to hydraulic fracturing. Although compositionally adequate for use as frac sands (particularly after increasing purity through washing processes), the median grain sizes in samples from the Plumbago Creek, John Blue Canyon, and Cassa deposits (99–197 µm) fail to meet criteria desirable for quality frac sands. However, silica sands ranging from 5 to 250 µm are commonly used as fillers and extenders for paint, rubber, plastic, and epoxy. Additionally, these sands may be useful for construction materials, foundry, filtration, or glass-making.

Dune Sand/Loess and Alluvial Fan Deposits

Dune sand deposits analyzed in this study have limited economic potential as frac sands. Samples from the Ferris-Seminoe and Sand Hills dunes failed to meet testing criteria for turbidity and are not suitable for hydraulic fracturing. Several samples from Killpecker dunes did not meet testing criteria based on either grain-size distribution, turbidity, acid solubility, and/or crush resistance. On the other hand, three samples showed marginal potential as proppant sand with crush resistance k-values of 3, 4, and 8 (appendix 2). The main issue at Killpecker Dunes is the variation in sand quality across the dune field. The lack of consistency across the area raises questions as to the reliability of these sands as a viable frac sand deposit.

Sands in the Casper Dunes did not meet testing criteria for either acid solubility or crush resistance. The alluvial fan deposit in the vicinity of the Casper Dunes, however, yielded k-values of 3 and 4. These sands may have potential for use in shallow hydraulic fracturing operations given their relatively low crush resistance, but further investigation is required to confirm the spatial extent of the deposit and the continuity of sand quality.

SUGGESTIONS FOR FUTURE WORK

The sands addressed in this study were evaluated with respect to their potential as hydraulic fracturing proppants. Further evaluation on these sands with a focus on standards for additional industrial uses will shed light on their potential in alternative markets. Additionally, the sands investigated for this report are not exhaustive of the sand-bearing geologic formations in Wyoming. Research into the geochemistry, physical properties, and spatial extent of other sand stone formations in the state may help identify additional silica sands and assess quality and quantity.

REFERENCES

Ahlbrandt, T.S., 1974, The source of sand for the Killpecker sand-dune field, southwestern Wyoming: Sedimentary Geology, v. 11, p. 39–57.

Ahlbrandt, T.S., 1973, Sand dunes, geomorphology, and geology, Killpecker Creek area, northern Sweetwater County, Wyoming: Laramie, University of Wyoming, Ph.D. dissertation, 174 p.

Ahlbrandt, T.S., and Fryberger, S.G., 1980, Eolian deposits in the Nebraska Sand Hills, chap. A of Geologic and paleoecologic studies of the Nebraska Sand Hills: U.S. Geological Survey Professional Paper 1120-A, 24 p.

Albanese, J.P., 1974, Geology of the Casper archeological site, in Frison, G.C., ed., The Casper Site, a Hell Gap bison kill on the high plains: Academic Press, New York, p. 174–190.

American Petroleum Institute, 2008, Measurement of properties of proppants used in hydraulic fracturing and gravel-packing operations—ANSI/API Recommended Practice 19C (1st ed.): Washington, DC, API Publishing Services, 30 p.

Bell, L.H., 1970, Depositional history of the Cambrian Flathead Sandstone, Park County, Wyoming, in Enyert, R.L., ed., Symposium on Wyoming sandstones: Wyoming Geological Association, 22nd annual field conference, Guidebook, p. 115–131.

Bellmund, Holly, 2017, Frac sand 101—What does it take to enter the high-value frac sand market and what does it mean for aggregate producers?, accessed September 2017, at https://www.aggman.com/frac-sand-101-what-does-it-take-to-enter-the-high-value-frac-sand-market-and-what-does-it-mean-for-aggregate-producers/.

Benson, M.E., and Wilson, A.B., 2015, Frac sand in the United States—A geological and industry overview: U.S. Geological Survey Open-File Report 2015-1107, 78 p.

Christiansen, W.D., and Anderson, B.C., 1982, Field report on the Rattlesnake Hills—Silica sand deposit, central Wyoming (unpublished): Burlington Northern Railroad, 64 p.

Darton, N.H., 1908, Paleozoic and Mesozoic of central Wyoming: Geological Society of America Bulletin, v. 19, p. 403–470.

Dolley, T.P., 2017, Mineral commodity summaries 2017: U.S. Geological Survey, p. 144–145, accessed March 2017, at https://minerals.usgs.gov/minerals/pubs/commodity/silica/mcs-2017-sandi.pdf.

Gaylord, D.R., 1982, Geologic history of the Ferris dune field, south-central Wyoming: Geological Society of America Special Paper 192, 18 p.

Gaylord, D.R., 1989, Field trip guide to the Ferris and Seminoe dune fields, in Gas resources of Wyoming: Wyoming Geological Association, 40th annual field conference, Guidebook, p. 269–276.

Gibbons, A.B., Barton, H.N., Kulik, D.M., and McDonnell, J.R., Jr., 1990, Mineral resources of the Buffalo Hump and Sand Dunes Addition wilderness study areas, Sweetwater County, Wyoming: U.S. Geological Survey Bulletin 1757-G, 22 p.

Harris, R.E., 1988a, The Plumbago Creek silica sand deposit, Albany County, Wyoming: Geological Survey of Wyoming [Wyoming State Geological Survey] Report of Investigations 40, 32 p.

Harris, R.E., 1988b, The Cassa silica rock deposit, Platte County, Wyoming: Geological Survey of Wyoming [Wyoming State Geological Survey] Report of Investigations 42, 38 p.

Harris, R.E., and Warchola, R.J., 1992, John Blue Canyon silica sand deposit, Big Horn County, Wyoming: Geological Survey of Wyoming [Wyoming State Geological Survey] Open File Report 92-3, 26 p., 1 pl.

Kolm, K.E., 1982, Predicting the surface wind characteristics of southern Wyoming from remote sensing and eolian geomorphology: Geological Society of America Special Paper 192, p. 25–53.

Kolm, K.E., and Marrs, R.W., 1977, Predicting surface wind characteristics of southern Wyoming from remote sensing and eolian geomorphology—Final report for contract EY-76-S-06-2343, University of Wyoming: Department of Energy Report RLO/2343-77/3, 142 p.

Krumbein, W.C., and Sloss, L.L., 1963, Stratigraphy and sedimentation (2d ed.): San Francisco, W.H. Freeman and Co., 660 p.

Loope, D.B., and Swinehart, James, 2000, Thinking like a dune field—Geologic history in the Nebraska Sand Hills: Great Plains Research, v. 10, no. 1, 35 p.

Love, J.D., and Christiansen, A.C., comps., 1985, Geologic map of Wyoming: U.S. Geological Survey, 3 sheets, scale 1:500,000. (Re-released 2014, Wyoming State Geological Survey.)

Lynds, R.M., Toner, R.N., Freye, A.M., Sutherland, W.M., and Loveland, A.M., 2016, Preliminary geologic map of the Ervay Basin SW quadrangle, Natrona County, Wyoming: Wyoming State Geological Survey Open File Report 2016-4, 31 p., 1 pl., scale 1:24,000.

Marrs, R.W., Kolm, K.E., and Gaylord, D.R., 1987, Dunes of the Wyoming wind corridor, southern Wyoming, in Beus, S.S., ed., Geological Society of America, Rocky Mountain Section, Centennial field guide 6 (2), p. 209–212.

Merewether, E.A., Kulik, D.M., and Ryan, G.S., 1987, Mineral resources of the Sand Dunes Wilderness Study Area, Sweetwater County, Wyoming: U.S. Geological Survey Bulletin 1757-A, 22 p.

Muhs, D.R., 2004, Mineralogical maturity in dunefields of North America, Africa and Australia: Geomorphology, v. 59, p. 247–269.

Stanley, K.O., and Wayne, W.J., 1972, Epeirogenic and climatic controls of early Pleistocene fluvial sediment dispersal in Nebraska: Geological Society of America Bulletin, v. 83, no. 12, p. 3675–3690.

Sutherland, Wayne, and Hausel, W.D., 2003, Geologic map of the Rattlesnake Hills 30' x 60' quadrangle, Fremont and Natrona Counties, Wyoming: Wyoming State Geological Survey Map Series 61, 1 sheet, scale 1:100,000.

Zdunczyk, Mark, 2014, Hydraulic fracturing sand (frac sand): Mining Engineering, v. 66, no. 7, p. 53–55.

Zdunczyk, Mark, 2007, The facts of frac: Industrial Minerals Journal, no. 1, p. 58–61.

Appendix 1

Disclaimer: The data in the appendix below are from an unpublished Burlington Northern Railroad (BNR) report (Christiansen and Anderson, 1982). BNR makes no representations about the current accuracy of the data presented or its value for any purpose beyond that for which it was prepared.

Table A1. Summary of physical characteristics of the Flathead Sandstone deposit at Rattlesnake Hills, Natrona County. Data from Christiansen and Anderson, 1982.

Sample ID	Flathead Designation	Location (PLSS)	Sample Description	Grain Size and Distribution	Grain Shape	Friability	Composition	Notes
BA-RS1-82	lower	T. 33 N., R. 88 W., sec. 8, NW/4SE/4NE/4	white, white-tan weathering, poorly-sorted, very coarse to fine-grained quartz arenite	grain sizes range from very coarse to fine-grained; weakly bimodal grain distribution with 1 node in very coarse size and other nodes in medium grain size; Rock is poorly-sorted and contains grains up to 4 mm in diameter.	subrounded to rounded grains with low to moderate sphericity	fair	quartz: 94%; feldspar: 5% (mostly going to clay); ferromagnesium: 1%	Some $MN0_2$ staining and some sulphur coating of grains
BA-RS2-82	lower-basal?	T. 32 N., R. 88 W., sec. 2, NE/4NE/4NW/4	gray-yellow, tan to light orange weathering, poorly-sorted, conglomeratic, arkosic sandstone	poorly-sorted; grain size ranges from 7 mm to fine grained (0.125–0.177 mm); fairly even size distribution throughout size range	angular to subrounded grains with low to moderate sphericity	moderate to poor	quartz:75%; biotite: 4%; muscovite: 2–3%; feldspar: 10%; ferromagnesium: 2%; lithic fragments: 5%	clay matrix between grains
BA-RS3-82	lower	T. 33 N., R. 87 W., sec. 31, SW/4NW/4SE/4	white-peach, brown-gray weathering, moderately-sorted, coarse- to fine-grained quartz arenite	coarse to medium-fine (0.177–0.350 mm) grains with bimodal distribution; majority of grains are of the smaller grain size	subrounded to well-rounded grains with moderate to high sphericity	very good	quartz: 98%; blue quartz: 2–3%; ferromagnesium: 1%; mica: trace	light hematite rinds on some grains
BA-RS4-82	lower	T. 32 N., R. 88 W., sec. 5, SE/4SW/4SW/4	white-pink, white-pink weathering, well-sorted, fine- to medium-grained friable quartz arenite	fine to medium grains with slight bimodal grain distribution; grains are medium-grained and fine-grained; majority of grains are fine-grained	subrounded to well-rounded grains with moderate to high sphericity	good to very good	quartz: 99%; magnetite: trace; feldspar(?): trace	some hematite banding present (minor)
BA-RS5-82	upper	T. 33 N., R. 88 W., sec. 6, NE/4SE/4SE/4	tan-gray, gray weathering, well-sorted, medium-grained quartz arenite	medium grains with unimodal grain distribution; large number of fines generated from overgrowths	subrounded to rounded grains with moderate sphericity	poor	quartz: 99%; ferromagnesium: trace	N/A
BA-RS6-82	lower	T. 33 N., R. 88 W., sec. 8, NW/4NE/4NW/4	light orange, light orange weathering	rock is moderately-sorted; trimodal grain size distribution; large majority of grains are medium-grained; small stringers of coarse grains; a third grain size concentration is in the fine grain size.	subrounded to well-rounded grains with moderate to high sphericity; larger grains are better rounded	good to very good	quartz: 99%; magnetite: 1%	some quartz grains have light hematite coatings

Table A1. cont.

Sample ID	Flathead Designation	Location (PLSS)	Sample Description	Grain Size and Distribution	Grain Shape	Friability	Composition	Notes
BA-RS7-82	lower	T. 33 N., R. 88 W., sec. 8, NE/4SE/4NE/4	white to light pink; white to red weathering, very well-sorted, fine-grained quartz arenite	very well-sorted with a unimodal grain size distribution; grains are fine; some coarse grains which are isolated within the fine-grained material	subrounded to rounded grains with low to moderate sphericity	good to very good	quartz: 99%; magnetite(?): trace	some pocketed hematite staining from decaying ferromagnesium
BA-RS8-82	lower	T. 33 N., R. 88 W., sec. 9, SW/4SE/4NW/4	gray to light orange, orange weathering, well-sorted, medium- to fine-grained quartz arenite	well-sorted (unimodal distribution) and medium- to fine-grained	subrounded to well-rounded grains with moderate to high sphericity; shell fragments are angular with low sphericity	fair	quartz: 97%; feldspar: trace; ferromagnesium: trace; shell fragments: 2–3%	some hematite banding
BA-RS9-82	lower	T. 33 N., R. 88 W., sec. 9, NW/4NE/4SW/4	pink, tan to red weathering; moderately-sorted, coarse- to fine-grained quartz arenite	grain sizes range from coarse to fine; grain size distribution is strongly bimodal; one mode is in the coarse size, the other in fine grain size; fine mode is the predominant mode	subrounded to well-rounded grains with moderate to high sphericity; fines tend to be more angular	good to very good	quartz: 97%; blue quartz: trace; feldspar: 2%; ferromagnesium: 1%; mica: trace	hematite coating on some grains
BA-RS10-82	upper	T. 33 N., R. 88 W., sec. 9, SW/4NW/4SE/4	tan-orange, red-brown weathering, well-sorted, medium-grained quartz arenite	medium (0.250–0.350 mm) grains with unimodal grain size distribution	subangular to subrounded grains with low to moderate sphericity	poor	quartz: 98%; feldspar: 1–2%; hematite: 1%	hematite appears to be a coating on the grains and also a pore filler (cement?); $MN0_2$ spots appear throughout the rock; noncalcareous shell fragments are also present
BA-RS11-82	lower	T. 33 N., R. 88 W., sec. 9, NE/4SW/4SE/4	white-pink, tan-orange weathering, well-sorted, medium- to fine-grained quartz arenite	rock is well-sorted with a bimodal grain size distribution; grains are concentrated in the medium (0.350–0.500 mm) and fine (0.125–0.177 mm) sizes; some coarse grains (0.500–0.710 mm) are present	subangular to rounded grains with moderate to high sphericity; small (fine) grains are generally subangular	good	quarts: 95%; feldspar: 3%; ferromagnesium: 2%; (amphibole)	some pocketed hematite due to ferromagnesium decay
BA-RS12-82	lower	T. 33 N., R. 88 W., sec. 9, SW/4SE/4SE/4	white-red, tan-red weathering, well-sorted, coarse- to fine-grained quartz arentite	grains range from coarse (0.710–1.00 mm) to fine (0.250–0.177 mm) in size; rock is well-sorted into these two sizes with a strongly bimodal distribution; majority of grains are fine in size	subrounded to well-rounded grains with moderate to high sphericity	good to excellent (some minor indurated ledges)	quartz: 99%	hematite spots possibly due to ferromagnesium decay; some ledges are heavily hematite stained

Table A1. cont.

Sample ID	Flathead Designation	Location (PLSS)	Sample Description	Grain Size and Distribution	Grain Shape	Friability	Composition	Notes
BA-RS13-82	lower	T. 33 N., R. 88 W., sec. 15, SE/4NW/4NW/4	white, tan-brown weathering, well-sorted, medium- to fine-grained, friable quartz arenite	medium (0.250–0.350 mm) to fine (0.250–0.177 mm) grains; unimodal distribution	subangular to rounded grains with moderate to high sphericity	very good	quartz: 97%; feldspar: 2–3%; amphibole(?): trace	n/a
BA-RS14-82	upper	T. 33 N., R. 88 W., sec. 15, NE/4SE/4NE/4	red-gray, red weathering, well-sorted, very fine-grained, glauconite, feldspathic quartz arenite	very fine (0.125–0.062 mm) grains with unimodal distribution	subangular to rounded grains with moderate to high sphericity; glauconite grains are usually more rounded	fair to poor	quartz: 85–90%; glauconite: 5%; feldspar: 5%: mica: 1–2%; ferromagnesium: trace	rock is hematite banded; also shows dolomite cement (possible groundwater movement from Buck Springs)
BA-RS15-82	lower	T. 33 N., R. 88 W., sec. 15, NW/4NE/4NE/4	white-pink, pink weathering, well-sorted, fine-grained quartz arenite	grain size ranges from coarse (0.710–0.500 mm) to fine-grained (0.177–0.250 mm); distribution is polymodal; majority of grains are fine grain size; a second small size concentration appears in the coarse grain size (0.710–0.500 mm); a third minor grain size concentration appears in the 1–4 mm grain size	subangular to well-rounded grains with low to high sphericity; larger grains are more rounded and have greater sphericity	good	quartz: 98%; red chert: trace; feldspar: 1%; ferromagnesium: 1%	some pocketed hematite spots from decaying ferromagnesium; evidence of hematite cement and some hematite banding; hematite coating on some quartz grains
BA-RS16-82	lower	T. 33 N., R. 88 W., sec. 14, SW/4SE/4SW/4	orange-brown, orange to light red weathering, well-sorted, coarse- to fine-grained quartz arenite	rock is well-sorted and exhibits a strongly bimodal grain size distribution; contains coarse (0.500–0.710 mm) and fine (0.177–0.250 mm) grains; majority of grains are fine	subrounded to well-rounded grains with moderate to high sphericity; larger grains are generally well-rounded	excellent	quartz: 99%; ferromagnesium: trace; mica: trace	light hematite coating on most quartz grains; some hematite pockets from decaying ferromanesium
BA-RS17-82	lower	T. 33 N., R.88 W., sec. 23, NW/4SE/4NE/4	white-pink, pink weathering, well-sorted, coarse- to fine-grained quartz arenite	rock is well-sorted and has a bimodal grain size distribution; grains are concentrated into the coarse-medium (0710–0.350 mm) and fine (0.125–0.177 mm) sizes	subrounded to well-rounded grains with moderate to high sphericity	very good except for some very small orthoquartzite lenses	quartz: 98%; feldspar: 1%; ferromagnesium: trace	n/a
BA-RS18-82	lower	T. 33 N., R. 88 W., sec. 25, NW/4NW/4NE/4	light brown to ruddy brown, tan-red weathering, moderately-sorted coarse- to fine-grained quartz arenite	rock is moderately-sorted with trimodal grain size distribution; grains are concentrated into coarse (0.710–1.000 mm), medium (0.350–0.500 mm), and fine (0.125–0.177 mm) grain sizes	subrounded to well-rounded grains with moderate to high sphericity; larger grains are more well-rounded	good to excellent	quartz: 99%; ferromagnesium: trace; feldspar: trace	light hematite coating on some grains; some hematite staining is present

Table A1. cont.

Sample ID	Flathead Designation	Location (PLSS)	Sample Description	Grain Size and Distribution	Grain Shape	Friability	Composition	Notes
BA-RS18a-82	lower	T. 33 N., R. 88 W., sec. 25, NW/4NW/4NE/4	yellow-brown, brown-red weathering, hematite-spotted, well-sorted coarse- to medium-grained quartz arenite	rock is well-sorted with a unimodal grain size distribution; grain size ranges from coarse (0.710–0.500 mm) to medium-grained (0.250–0.400 mm); majority of the grains are medium size	grains are well-rounded with moderate to high sphericity	excellent	quartz: 97% +/-; decayed ferromagnesium: 3%	pocketed hematite staining comes from decaying ferromagnesium minerals; red clay particles are present in the rock; some grains have light hematite coating
BA-RS19-82	lower	T. 33 N., R. 88 W., sec. 25, NE/4NW/4SE/4	light orange-red, light orange-red weathering, very well-sorted, medium-grained quartz arenite	rock is very well-sorted (unimodal distribution) in the medium grain size (0.250–0.350 mm)	rounded to well-rounded grains with moderate to high sphericity	good	quartz: 99%; feldspar: trace	light hematite coating on grains; hematite pore (?) filling in some places (hematite cement); non-calcarous shell fragments in some coarser layers
BA-RS-20-82	undifferentiated	T. 33 N., R. 87 W., sec. 31, NE/4SW/4NW/4	white, tan, tan weathering, well-sorted, medium- to fine-grained quartz arenite	grain sizes range from medium (0.500–0.350 mm) to fine (0.177–0.125 mm); stongly bimodal distribution of grains in these two size categories; majority of grains are fine	subangular to rounded grains with moderate sphericity	very good	quartz: 98%; ferromagnesium: 1%; feldspar: trace	n/a
BA-RS21-82	lower	T. 33 N., R. 88 W., sec. 7, NW/4NW/4NE/4	light tan, light tan to light orange weathering, well-sorted, medium- to fine-grained quartz arenite	rock is well-sorted with a bimodal distribution; grain sizes range from medium (0.350–0.500 mm) to fine (0.125–0.177 mm); grain size concentrations are present in the medium and fine grain sizes	coarser grains are rounded to well-rounded with high sphericity; fine grains are subangular to subrounded with low to moderate sphericity	variable; some ledges are very friable; upper ledges of outcrop are very hard orthoquartzite	quartz: 97%; ferromagnesium: 1–2%; feldspar: 1%	some pocketed hematite (ferromagnesium decay)
BA-RS22-82	lower	T. 33 N., R. 88 W., sec. 7, SE/4SE/4NE/4	yellow-pink, brown weathering, very well-sorted, medium-grained quartz arenite	medium (0.350–0.500 mm) sized grains with unimodal distribution	subangular to rounded grains with moderate to high sphericity	good	quartz: 99%	angularity of some grains bay be due to overgrowths; light hematite coating on some grains
BA-RS23-82	lower	T. 33 N., R. 88 W., sec. 7, SE/4 SE/4 NE/4	orange, orange-brown weathering, moderately sorted coarse- to fine-grained quartz arenite	rock is moderately-sorted and has a bimodal grain size distribution; grains are concentrated in the coarse-medium (0.350–0.710 mm) and fine (0.125–0.177 mm) grain sizes	subrounded to well-rounded grains with moderate to high sphericity	very good	quartz: 99%; ferromagnesium: 1%	n/a

Table A1. cont.

Sample ID	Flathead Designation	Location (PLSS)	Sample Description	Grain Size and Distribution	Grain Shape	Friability	Composition	Notes
BA-RS24-82	lower	T. 33 N., R. 88 W., sec. 17, SE/4NW/4NE/4	white-pink, pink-brown weathering, well-sorted, coarse- to fine-grained quartz arenite	rock is well-sorted and displays strong bimodal grain size distribution; grains are concentrated into the coarse (1.000–0.500 mm) and fine (0.250–0.125 mm) sizes	coarse grains are rounded to well-rounded with high sphericity; fine grains are subangular to rounded with low to moderate sphericity	good	quartz: 99%	rock contains some grains up to 3.5 mm in size
BA-RS26-82	lower	T. 33 N., R. 88 W., sec. 16, NW/4SW/4NW/4	orange, tan-brown weathering, well-sorted, coarse- to medium-grained quartz arenite	rock is well-sorted and displays unimodal grain size distribution; grains are coarse (0.710–0.500 mm) to medium (0.500–0.350 mm) in size	grains are subrounded to well-rounded with moderate to high sphericity	good	quartz: 99% (some smokey quartz)	pervasive hematite staining gives rock a light orange color
BA-RS-27-82	lower	T. 33 N., R. 88 W., sec. 17, SW/4NE/4NE/4	white-tan, light brown weathering, moderately well-sorted, medium- to fine-grained quartz arenite	rock is moderately well-sorted and exhibits strongly bimodal grain size distribution; grains are concentrated into the medium (0.350–0.500 mm) and fine (0.177–0.250 mm) grain sizes; majority of grains are fine grain size	subangular to rounded grains with moderate to high sphericity; larger grains are better rounded; fine grains are subangular to subrounded	good to very good	quartz: 99%; rose quartz: trace	n/a
BA-RS28-82	lower	T. 33 N., R. 88 W., sec. 16, SW/4SE/4NW/4	light orange-white, brown weathering, moderately-sorted, coarse- to fine-grained, well-indurated orthoquartzite	rock is moderately-sorted with bimodal grain size distribution; grains are concentrated into the coarse (0.710–0.500 mm), medium (0.500–0.350 mm), and fine (0.250–0.125 mm) sizes	subangular to rounded with moderate sphericity	very poor (well-indurated)	quartz: 99%	rock is highly silicified and fine grains are at times indestinguishable; rock breaks through grains
BA-RS29-82	lower	T. 33 N., R. 88 W., sec. 35, SE/4NE/4SW/4	light orange-red, light orange-brown weathering, well-sorted, fine-grained quarz arenite	rock is well-sorted with unimodal grain size distribution in the fine (0.177–0.250 mm) grain size; some coarse to medium grains are present in the fine material	subangular to rounded grains with low to moderate sphericity	very good	quartz: 97%; feldspar: trace; ferromagnesium: 2–3%; pyroxene (?)	light hematite coatings on some grains
BA-RS29a-82	lower	T. 33 N., R. 88 W., sec. 35, SE/4NE/4SW/4	tan, light brown weathering, very well-sorted, coarse-grained quartz arenite	rock is very well-sorted, and has a unimodal grain size distribution; grains are coarse (0.710–0.500 mm) in size	grains are rounded to well-rounded and have high sphericity	good	quartz: 99%	light hematite coating on some grains
BA-RS30-82	lower	T. 33 N., R. 88 W., sec. 35, NW/4NE/4SW/4	yellow-white, white weathering, poorly-sorted, coarse- to very fine-grained quartz sandstone	rock is poorly sorted with grains ranging in size from coarse (1.000–0.710 mm) to very fine (0.088–0.125 mm); polymodal grain size distribution	angular to subrounded grains with low to moderate sphericity	good	quartz: 90%; feldspar: 6%; mica: 3%; ferromagnesium: 1%	a basal(?) unit is also present with a lithology very similar to BA-RS2-82

Appendix 2

Table A2. Summary of crush resistance and/or acid solubility analyses performed by Legend Technical Services, Inc.

	Sample	Location	Formation	Sample Preparation	Loss After Washing (%)	Raw Washed Yield (%)	Bulk Density (metric) gr/ft3	Bulk Density (U.S.) lb/cm3	Sphericity[1]	Roundness[2]	Acid Solubility[3] (%)	Applied Load (in psi at 4.0 lbs/ft2)	Resulting Fines[4] (%)	Comments
Initial Results	20160628AML004	Killpecker Dunes	dune sand/ loess	Washed and sieved to a 40/70 cut	9.7	90.3	1.52	94.89	0.872	0.889	Not tested	4,000	6.1	The sand would be considered a 4k sand. Additional cut from the raw sand, such as a 100+ material, is feasible.
												5,000	10.6	
												5,000 (duplicate)	11.2	
	20160628AML006	Killpecker Dunes	dune sand/ loess	Washed and sieved to a 40/70 cut	6.23	93.77	1.48	92.39	0.864	0.882	Not tested	5,000	4.09	The material meets crush strength requirements for an 8k sand. The sand could also produce a 70/140 cut or a 100+ material.
												7,000	7.2	
												8,000	9.8	
	20160721AML007	Casper Dunes	dune sand/ loess	Washed and sieved to a 6/12 cut	31.51	68.5	1.35	84.28	0.865	0.895	Not tested	1,000	35.08	The material is an agglomeration of fine sand particles and clay. It crushes at less than 1,000 psi. If crushed, the material consists of fine aggregated sands which are too fine for use.
												3,000	48.5	
	20160721AML009	Casper Dunes	alluvial fan	Washed and sieved to a 40/70 cut	43.46	56.54	1.35	84.28	0.838	0.864	Not tested	4,000	7.82	The material meets the crush strength requirements for a 4k sand.
												5,000	10.82	
												6,000	14.9	
Results from Additional Samples	20170606AML001	Casper Dunes	dune sand/ loess	Washed	32.03	67.97	1.43	89.27	0.881	0.892	4.1	Not tested	n/a	The material failed the acid solubility testing. The sample had a significant amount of hematite nodules. Based on the failed acid solubility the material was not screened to size and was not tested for strength.
	20170607AML004	Casper Dunes	alluvial fan	Washed and sieved to a 70/140 cut	25.46	74.54	1.49	93.02	0.876	0.884	2.8	3,000	6.9	The material is a 3k sand. The sand contains a significant amount of hematite, which is primarily responsible for the low strength.
												4,000	12.6	
	20170622AML008	Killpecker Dunes	dune sand/ loess	Washed	37.2	62.8	1.51	94.27	0.884	0.899	3.88	Not tested	n/a	Since the sand failed solubility testing, it was not tested for strength. The sand contains a significant amount of hematite, which is primarily responsible for failing acid solubility.
	20170622AML011	Killpecker Dunes	dune sand/ loess	Washed and sieved to a 40/70 cut	23.96	76.04	1.5	93.64	0.883	0.896	2.92	3,000	6.5	The sand is a 3k sand. The sand contains a significant amount of hematite, which is primarily responsible for low strength. The elevated levels of hematite are responsible for the high acid solubility.
												4,000	14.1	
	20170623AML012	Killpecker Dunes	dune sand/ loess	Washed	2.7	97.3	1.57	98.01	0.88	0.896	4.1	Not tested	n/a	The sand contains hematite, which is primarily responsible for the high acid solubility.

[1] ISO 13503-2 limit for sphericity is ≥7.0; [2] ISO 13503-2 limit for sphericity is ≥7.0; [3] ISO 13503-2 limit for acid solubility is <3.0 percent; [4] ISO 13503-2 limit for fines is 10 percent

STATE OF WYOMING GEOLOGICAL SURVEY 1933

Interpreting the past, providing for the future

ISBN: 978-1-884589-61-4